ONLINE JOURNAL OF BIOLOGICAL SCIENCES

RESEARCH ARTICLE

Virtual Screening of Bioactive Compounds from the Onion (*Allium*) Genus as Potential Epidermal Growth Factor Receptor Inhibitors for Monkeypox

Dinda Ratu Agustiani, Rakhmat Ramdhani Alwie, Harry Noviardi*

Department of Pharmacy, Sekolah Tinggi Teknologi Industri dan Farmasi Bogor, Bogor 16128, West Java, Indonesia

*Corresponding Author: harry.noviardi@gmail.com

Abstract: Monkeypox (Mpox) is an emerging zoonotic disease caused by the Mpox virus infection that affects humans and animals. Epidermal Growth Factor Receptor (EGFR) is an important target in the pathogenesis of Mpox. Epidermal Growth Factor (EGF), encoded by orthopoxviruses, plays an important role in intercellular transmission of the virus. Onion is known to have antiviral and immunomodulatory properties. Active compounds in onions, such as allicin and flavonoids, have the potential to inhibit viral replication, such as in adenovirus. This research aims to identify the potential of bioactive compounds in plants of the *Allium* genus, consisting of *Allium sativum* L., *Allium cepa* L., *Allium ascalonicum* L., and *Allium schoenophrasum* L., as EGFR inhibitors using an in silico approach. Compounds from plants of the onion genus were tested with binding affinity (ΔG), inhibition constant (Ki), physicochemical, toxicity, Absorption, Distribution, Metabolism, Excretion (ADME), structure-activity relationship, and molecular dynamics parameters. From 1030 plant compounds of the onion genus, the compound 2-(3,4-dihydroxyphenyl)-5- hydroxy-4-oxo-4H-chromen-7-olate luteolin-7-olate(1-) was obtained from plants. *Allium sativum* L. has the potential as an EGFR inhibitor with a binding affinity (ΔG) value of -8.8 kcal/mol and a Ki of 0.966 µM. Molecular weight of 285 Daltons, 3 hydrogen donors, 6 hydrogen acceptors, log P partition coefficient value of 1.650, good ADMET and structure-activity relationship, and total energy molecular mechanics Generalized Boltzmann Surface Area (MM-GBSA) of 22.69 kcal/mol.

Keywords: *Allium,* EGFR, Monkeypox, Virtual Screening, Inhibitor

Received: 07-01-2026 | **Revised:** 18-05-2026 | **Accepted:** 15-06-2026 | **DOI:** 10.3844/ojbsci.2026.26.03.060

Introduction

Monkeypox (Mpox) is an emerging zoonotic disease caused by the viral infection Mpox, which attacks humans and animals [1]. This virus was first found in monkeys in 1958 and has since been detected in various animal genera. The first case of mpox infection in humans was diagnosed in 1970 in the Republic of Congo, located in Central Africa [2]. In addition, Mpox circulates mainly in Central and West Africa, with transmission occurring between animals (especially primates and rodents), as well as between animals and humans, and through human-to-human contact [3]. Notably, in 2022, the global epidemic of Mpox affected 110 countries and territories [4]. Since May 2022, there has been a significant increase in the number of cases of monkeypox throughout Europe and other nations. As of August 5, 2022, there were 26,017 confirmed

cases of monkeypox and 9 fatalities (mortality rate <0.0005%). Over 75 nations in six WHO geographical divisions have reported cases [5].

Epidermal Growth Factor Receptor (EGFR) is a tyrosine kinase receptor that controls the process of cellular homeostasis [6]. The EGFR plays an important role in the development of Mpox. Epidermal Growth Factor (EGF), encoded by orthopoxviruses, plays an important role in the transmission of viruses between cells [7]. EGF has the ability to activate the EGFR/MEK (Mitogen-Activated Protein Kinase)/FAK (Focal Adhesion Kinase) pathway, which promotes viral transmission between cells and accelerates the movement of infected cells [8]. Although EGFR is not a viral enzyme, its role in viral dissemination makes it an indirect but promising host-targeted strategy.

Compounds of epidermal growth factor receptor inhibitor (EGFR) showed promising antiviral activity against the monkeypox virus in addition to its approved indications for late-stage non-small cell lung cancer. An example of a drug compound from the EGFR inhibitor group used for treatment of Mpox is gefitinib. By using this inhibitor, there are limitations related to resistance. Therefore, the development of new, more effective inhibitors is very important to overcome this problem [9].

Onions are known to have antiviral and immunomodulatory properties. Active compounds in onions, such as allicin, flavonoids, and sulfur compounds, have the potential to inhibit viral replication, such as in adenovirus [10]. Some studies show that onions can provide a protective effect against various viral infections, especially through inhibitory mechanisms on signaling pathways involving Epidermal Growth Factor Receptor (EGFR). Research shows that onion extract can inhibit viral replication by disrupting signaling pathways involving EGFR, thereby reducing the virus's ability to infect. Although EGFR is not a viral enzyme, its involvement in viral dissemination and infected-cell migration makes EGFR inhibition a biologically relevant host-targeted strategy against Mpox infection [11].

Compounds in onions can modulate EGFR expression and disrupt signaling pathways necessary for viral replication. By inhibiting EGFR, onions can reduce the virus's ability to infect and multiply in host cells [11]. Although direct research on the effects of onions on the monkeypox virus is still limited, the antiviral properties of onions provide hope for the development of plant-based therapies.

In silico drug design may be utilized to ascertain the three-dimensional configuration of both the active compound and the target enzyme. The docking procedure may forecast compounds that function as inhibitors, thus enhancing the efficiency of the screening and experimental testing procedure. This investigation was conducted in silico utilizing the molecular docking and molecular dynamics approach within the framework of molecular modeling. Molecular modeling was utilized to develop and illustrate the structure and properties of specific compounds through computational chemistry techniques and graphical visualization [12, 13].

Plants from the genus Allium are significant sources of bioactive chemicals, including flavonoids and organosulfur compounds, which have been found to have antiviral and immunomodulatory properties and to alter EGFR-related signaling pathways. However, recent studies generally target their anticancer or broad-spectrum antiviral characteristics, while comprehensive investigations of Allium-derived compounds as EGFR inhibitors in the context of Mpox infection are still scarce. Furthermore, the molecular mechanism behind their interaction with EGFR and their potential relevance as host-targeted antiviral options remain inadequately investigated. In addition, most published in silico investigations rely solely on molecular docking, without comprehensive validation employing molecular dynamics simulations, MM-GBSA binding free energy calculations, and integrated pharmacokinetic and toxicity (ADMET) assessments. Consequently, the stability of Allium-derived compound–EGFR complexes under physiological settings and their drug-likeness profiles have not been extensively studied. This study aims to address these gaps by applying an integrated in silico approach to identify and characterize potential EGFR inhibitors from the Allium genus, thereby providing a rational foundation for further experimental validation and the development of novel host-targeted therapeutic strategies against Mpox. An increase in the RMSD value suggests that the receptor structure is beginning to open and the ligand is starting to hunt for acceptable binding sites or locations on the protein.

Materials and Methods

Materials

The three-dimensional structure of the protein Epidermal Growth Factor Receptor (EGFR) complexed with gefitinib was downloaded from the RSCB database site Protein Data Bank (https://www.rscb.org/) with code 4WKQ. A total of 1069 three-

dimensional structures of bioactive compounds of Allium sativum L., Allium cepa L., Allium ascalonicum L., and Allium schoenophrasum L., as well as the comparative ligand gefitinib, can be downloaded from the database PubChem in *.sdf format.

Tool

Hardware computer with operating system Windows 10 Pro and 64 GB RAM. Molecular docking simulation using AutoDock Tools version 1.5.7, Discovery Studio Visualizer version 21.1.0, AutoDock Vina version 1.1.2, PyMOL version 2.5.4, DataWarrior version 5.5.0, the online program of pkCSM, and Desmond version 5.1.1.

Methods

Molecular Docking Analysis

The EGFR structure (Epidermal Growth Factor Receptor) from PDB was downloaded in *.pdb format. The resolution and plot are viewed on the receptor Ramachandran via PDBsum to determine the feasibility of the receptor in carrying out the molecular docking process. Test ligand collection was carried out by downloading the compound structures that will be used for docking via the PubChem site. For separating proteins and ligands, removing water molecules, and adding hydrogen to macromolecules before molecular docking, PyMOL version 2.5.4 was used.

AutoDock Tools was used to optimize EGFR molecules that have been separated from residues. This optimization includes several parameters, such as the addition of hydrogen atoms and settings for the grid box (x = 24, y = 28, z = 28), spacing (0.608 Å), and grid box center (x = 3.062, y = 192.506, z = 22.123). Before molecular docking is carried out, the molecular docking method is internally validated by comparing the structural model of the target protein with the ligand gefitinib. After validation of the molecular docking method, the same parameters are used for docking all test ligands with EGFR using AutoDock Vina [14]. The docking results were evaluated and visualized using Discovery Studio Visualizer version 21.1.0 [15].

Test Lipinski's Rule of Five and ADMET

Predicting physicochemical properties and pharmacokinetic and toxicity properties (ADME: absorption, distribution, metabolism, excretion) was carried out via the pkCSM website using simplified molecular-input line-entry system (SMILES) ligands to be predicted [16].

Determination of the Relationship between Ligand Structure and Biological Activity

Determination of the structural activity relationship of ligands with the EGFR protein was based on canonical SMILES and its binding energy using DataWarrior version 5.5.0 software. The aim is to determine how molecular descriptors correlate with the biological activity of the test compounds and predict their activity [17].

Molecular Dynamics Simulation

Molecular dynamics simulations between the EGFR protein and the best test compound were carried out for 100 nanoseconds using Desmond version 5.1.1. The initial stage of the protein and ligand complex for molecular dynamics simulation was obtained from molecular docking. The simulation was carried out to predict the ligand binding status from time to time in a physiological environment [18].

Results and Discussion

Epidermal Growth Factor Receptor (EGFR) was downloaded from the Protein Data Bank (PDB) with PDB ID code 4WKQ and has a resolution value of 1.85 Å. EGFR forms a complex with the comparison ligand gefitinib, 2-(N- Morpholino)-Ethanesulfonic acid, sodium ions, and water molecules. The protein macromolecule receptor that forms a complex with the ligand and solvent was separated using the application Discovery Studio Visualizer 2021. Water molecules that form a complex with the 4WKQ receptor were removed because they can affect the virtual screening results, making virtual screening less than optimal. In the protonation phase, a hydrogen atom was added to stabilize the bond and adjust the body's biological pH to pH 7.4.

The selection of suitable receptors can be seen from the Ramachandran plot (Figure 1). The Ramachandran diagram consists of four quadrants, namely most favored regions, additional allowed regions, generously allowed regions, and

DOI: 10.3844/ojbsci.2026.26.03.060

disallowed regions. 4WKQ is a stable and high-quality receptor. This is indicated by the percentage of amino acid residues in most favored regions of 90.6% and disallowed regions of 0.4%. The higher the percentage of amino acid residues that are in the most preferred region (most favored regions) and the lower the percentage of amino acid residues in the disallowed region (disallowed regions), the better the quality and stability of the structure [19].

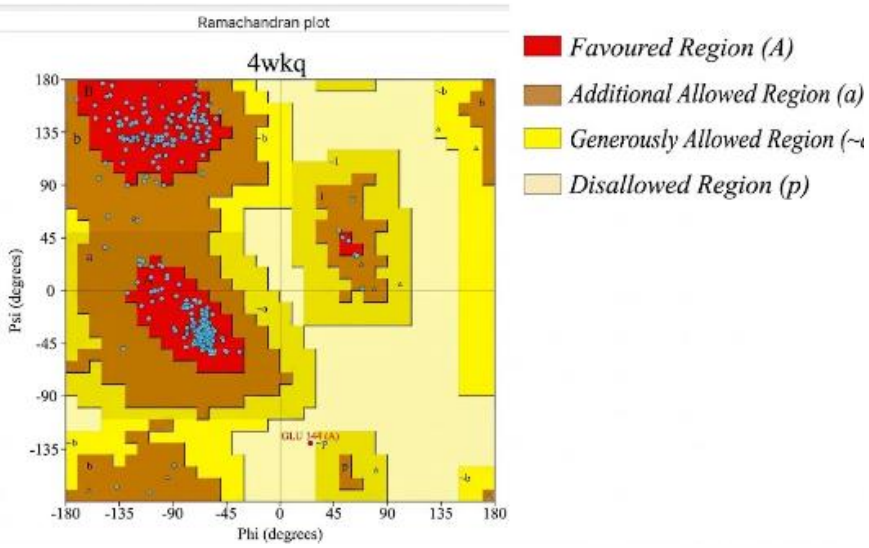

Fig. 1: Ramachandran Plot Receptor 4WKQ

Virtual Screening Method Validation

The molecular docking method validation process is carried out to ensure that this method is valid and can be used to test ligands and to reduce errors. If the RMSD value is less than 2 Å, the docking validation is considered valid. PyMOL is used to validate the docking method [13]. AutoDock Vina was chosen for its reliable prediction accuracy for protein–ligand interactions, efficient optimization algorithm, and improved scoring function, which have made it one of the most extensively validated docking tools in structure-based drug discovery. The ligands analyzed included the comparison ligand and the ligand that was already docked in the *.pdbqt format. Gefitinib is used to validate the virtual docking method because although gefitinib's effectiveness in treating Mpox is not yet known, gefitinib can reduce actin tail formation by 1.6-fold and decrease the migration efficiency of infected cells by up to four times [20]. The results of the molecular redocking of gefitinib to the 4WKQ protein resulted in an RMSD value of 1.545 Å and a binding affinity value of -7.9 kcal/mol, which indicates that the smaller the RMSD value, the closer it is to the position of the natural ligand resulting from docking with the natural ligand resulting from crystallography [21]. The test ligand docking simulation was carried out on the Epidermal Growth Factor Receptor (EGFR) (PDB Code: 4WKQ) receptor. The parameters used were the grid box parameters, which were the same as the validation parameters for the molecular docking method. The bond between the ligand and the EGFR protein (PDB Code: 4WKQ) can be seen from the binding affinity parameter, also known as Gibbs free energy (ΔG), as shown in Table 1, namely the ligand bond with the lowest binding affinity value.

The smaller the free energy value (ΔG), the greater the ability of a compound to bind to the receptor [12]. The binding affinity *value* is obtained from the bonds formed by the ligand. From Table 1, it can be seen that the test ligand 2-(3,4-dihydroxyphenyl)-5-hydroxy-4-oxo-4H-chromen-7-olate luteolin-7-olate(1-) has a binding affinity value that is the most negative or lowest compared to the gefitinib comparison ligand, which is -8.8 kcal/mol, so it is predicted that the test ligand has the potential to be an EGFR inhibitor. In this study, compounds showing docking scores below −7.0 kcal/mol and lower than the reference ligand were categorized as potential hit compounds, indicating favorable ligand–receptor binding stability.

Binding affinity is positively related to the value of the inhibition constant (Ki). The value of the inhibition constant (Ki) reflects the concentration required to achieve 50% inhibition. The smaller the Ki value, the stronger the ligand's affinity for macromolecules [13]. Based on the test ligand in Table 1, the smallest Ki value is owned by the test ligand 2-(3,4-dihydroxyphenyl)-5-hydroxy-4-oxo-4H-chromen-7-olate-luteolin-7-olate(1-) of 0.966 µM compared to the Ki value of the gefitinib comparison ligand of 0.970 µM, which is higher.

Table 1: Virtual Screening Results

No	Compound name	Plant origin	ΔG (kcal/mol)	Ki (μM)	Interaction With Amino Acids	
					Hydrogen bond	Hydrophobic bond
1	Gefitinib	Comparison compound	-7,9	0,970	Met 793 Gln 791 Thr 854 Asp 800 Pro 794	Met 766 Leu 788 Lys 745 Val 726 Leu 792 Leu 718 Leu 844 Ala 743 Glu 762
2	2-(3,4-dihydroxyphenyl)-5-hydroxy-4 -oxo-4H-chromen-7-olate luteolin-7-olate (1-)	*Allium sativum* L.	-8,8	0,966	Thr 854 Glu 762	Val 726 Ala 743 Lys 745 Thr 790

Bold text: indicates the best value

Analysis of molecular interactions can reveal specific relationships between ligands and receptors. These interactions are stabilized by hydrogen bonds and hydrophobic interactions. The energy resulting from hydrogen bonds is usually more significant than the energy from hydrophobic bonds, because hydrogen bonds have a large influence in determining the value of binding affinity during the docking process. The more hydrogen bonds that form with amino acid residues, the stronger and more stable the bond will be [22]. Judging from the virtual docking results of the ligand and target protein in Table 1, the gefitinib comparison ligand has 5 hydrogen bonds, including Met793, Gln791, Thr854, Asp800, and Pro794. In addition to hydrogen bonds, the gefitinib comparison ligand also has 9 hydrophobic bonds, including Met766, Leu788, Lys745, Val726, Leu792, Leu718, Leu844, Ala743, and Glu762. Based on the virtual docking results of the ligand and target protein in Table 1, the test ligand 2-(3,4-dihydroxyphenyl)

-5-hydroxy-4-oxo-4H-chromen-7-olate luteolin-7-olate(1-) has 3 hydrogen bonds, including Thr854, Glu762, and Csx797, and also has 4 hydrophobic bonds, including Val726, Ala743, Lys745, and Thr790. Compared to the interaction of the ligand and target protein between the gefitinib comparison ligand and the test ligand 2-(3,4- dihydroxyphenyl)-5-hydroxy-4-oxo-4H-chromen-7-olate-luteolin-7-olate (1), the test ligand only has 1 identical hydrogen bond, namely at the amino acid residue Thr854, and has 3 identical hydrophobic bonds, namely Val726, Ala743, and Lys745. These amino acid residues indicate that the test ligand 2-(3,4-dihydroxyphenyl)-5-hydroxy-4-oxo- 4H-chromen-7-olate luteolin-7-olate(1-) has an almost similar docking position to the EGFR inhibitor, gefitinib, although only a few amino acids can interact in the binding site. Thus, it can be predicted that the test compound 2-(3,4- dihydroxyphenyl)-5-hydroxy-4-oxo-4H-chromen-7-olate-luteolin-7-olate(1-) has better inhibitory activity on the EGFR receptor compared to other test ligands.

Lipinski's Rule of Five

In the development of new drugs, it is important to pay attention to solubility and permeability to prevent failure due to low drug absorption. Prediction of physicochemical parameters such as solubility and permeability is carried out based on the rules of Lipinski's Rule of Five. This rule is a prediction method in silico, which assesses the suitability of a chemical structure as a drug candidate for oral use, with conditions that must be met. These conditions include lipophilicity (C Log P) not more than 5, the number of hydrogen bond donors not more than 5, the number of hydrogen bond acceptors not more than 10, and the Molecular Weight (MW) not exceeding 500 g/mol [23]. In Table 2, test ligands that meet Lipinski's rules are shown, which can be predicted to have good absorptivity for use as an oral preparation.

Test compounds that do not adhere to the rules of Lipinski are not recommended for use as oral preparations. This is primarily due to the fact that a molecular weight exceeding 500 g/mol poses challenges for penetration through the digestive membrane. Additionally, the number of hydrogen bond donors suggests that a higher hydrogen bonding capacity correlates with an increased energy requirement for the absorption process to occur [12].

Pharmacokinetics and Toxicity

The pharmacokinetic, or ADME, parameters used in absorption are intestinal absorption in humans and skin permeability; in distribution, these include VDss in humans and blood-brain barrier permeability; in metabolism, they are CYP3A4 substrate

and CYP3A4 inhibitor; and in excretion, they are total clearance and renal OCT2 substrate. In toxicity testing, the parameters used include AMES toxicity, oral rat acute toxicity (LD_{50}), and hepatotoxicity. The ADMET test results for the test ligand and the reference ligand can be seen in Table 3.

Table 2: Analysis Results: *Lipinski* Plant Compounds of the Genus *Allium*

No	Ligand Name	Plant Origin	*Lipinski's rule of five*				Result
			MW	H Donor	H Acceptor	Log P	
1	Gefitinib	-	447	3	5	4,276	✓
2	2-(3,4-dihydroxyphenyl)- 5-hydroxy-4 -oxo-4H-chromen-7-olate luteolin-7- olate (1-)	*Allium* sativum L.	285	3	6	1,650	✓

Note: (✓) meets the requirements of Lipinski's Rule of Five

Table 3: ADMET Test Results

No	Parameter	Test Ligand		Interpretation
		Gefitinib	**2-(3,4-Dihydroxyphenyl)-5-hydroxy-4-oxo-4H-chromen-7-olate luteolin-7-olate(1-)**	
1	Intestinal absorption (human) (%)	90,99	76,10	Good
2	Skin Permeability (log Kp)	-2,75	-2,74	Acceptable
3	VDss (human) (log L/kg)	1,08	0,78	Good
4	BBB permeability (log BB)	-0,74	-0,71	Acceptable
5	CYP3A4 inhibitor (Yes/No)	No	No	Good
6	Total Clearance (log ml/min/kg)	0,94	0,41	Acceptable
7	Renal OCT2 substrate	No	No	Good
8	AMES toxicity (Yes/No)	No	No	Good
9	Oral Rat Acute Toxicity (LD_{50}) (mol/kg)	2,86 (1.278 g/kg) class 6	2,39 (682,84 g/kg) class 6	Good
10	Hepatotoxicity (Yes/No)	Yes	No	Good

Oral Drug Absorption: Mostly absorbed by the intestines. Good absorption value: > 80%; poor absorption value: < 30% [24]. The test ligands showed an absorption value > 30%, indicating good absorption. Although the intestinal absorption of the selected compound was lower than gefitinib, the value remained within the range considered favorable for oral absorption and therefore may still support acceptable oral bioavailability. Skin Permeability: Compounds with log Kp > -2.5 have good skin permeability [16]. The test ligands meet this criterion, making them suitable for transdermal administration. Volume of Distribution (VDss): A high VDss value (>0.45) indicates greater distribution into tissues compared to plasma [16]. The test ligand has a VDss value > 0.45, suggesting that drugs with a high Vd tend to leave the plasma and enter the body's extravascular compartments, meaning that higher drug doses are needed to achieve a specific plasma concentration [16]. Blood-Brain Barrier Penetration Ability: A log BB value >0.3 indicates the ability to penetrate the blood-brain barrier [16]. The test ligand has a log BB value > -1, suggesting that the test ligand can penetrate the blood-brain barrier evenly. Cytochrome P450 Enzyme: Important for drug metabolism [16]. The test ligand did not inhibit the cytochrome P450 isoform CYP3A4. Therefore, it can be predicted that the test ligand is likely to be metabolized by the P450 enzyme. Total Clearance (CLtot): Describes bioavailability and the required dose [16]. The test ligand showed a lower total clearance value compared to gefitinib. Transporter OCT (Organic Cation Transporter) 2: Plays a role in drug absorption and clearance [16]. The test ligand does not affect the OCT2 substrate, so it is predicted that there is no risk of adverse interactions. Toxicity Prediction: Using

LD_{50}, Ames toxicity, and hepatotoxicity tests. The test ligand has an LD_{50} category of class 6 and is predicted to be practically non-toxic, non-mutagenic, and non-hepatotoxic.

Relationship between Ligand Structure and Biological Activity

The relationship between ligand structure and biological activity aims to predict the activity of test compounds and understand the influence of molecular descriptors on their biological activity [25]. In this study, the analysis of the relationship between ligand structure and the EGFR protein is based on canonical SMILES and binding affinity, as shown in Figure 2. Figure 2 illustrates the correlation between the structural similarity of canonical SMILES (data points connected by colored lines) and binding affinity (circular data points with various colors) for the 7 test ligands. Structurally similar test ligands are grouped within dashed lines, and representative molecules with low binding affinity (kcal/mol) are enclosed in boxes [26]. Two test ligands out of seven, including flavon-type flavonoids with a binding affinity of -8.4 kcal/mol, showed that the addition of an O- ion to the side chain of the test ligand kaempferol oxoanion did not affect the binding affinity value. Meanwhile, in the test ligand, naringenin showed no structural similarity to the other 6 test ligands, as evidenced by one aromatic ring that was not proportional to the other aromatic ring and one heterocyclic ring. Consequently, the binding affinity value also differed, being -8.2 kcal/mol.

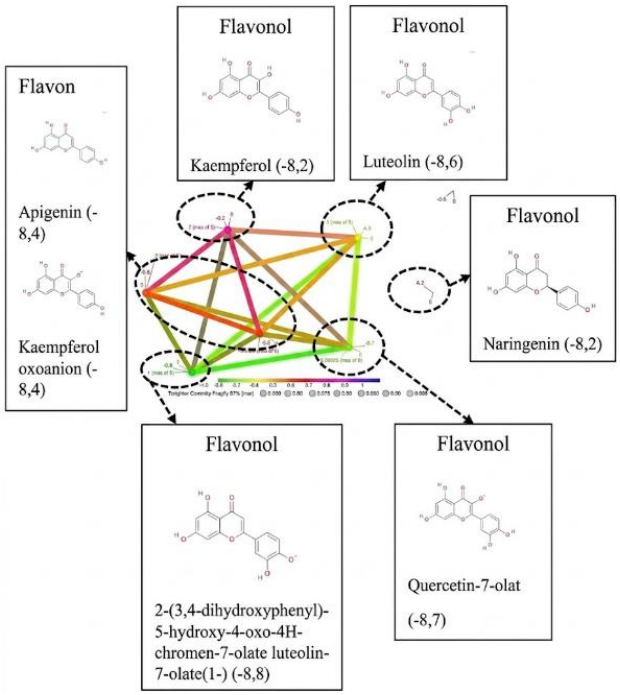

Fig. 2: Relationship between Structure and Biological Activity

Molecular Dynamics

Molecular dynamics simulation aims to analyze the stability of protein-ligand interactions created under conditions as similar as possible to the human body's physiological state within a specific timeframe [27]. The ligands analyzed are the test ligand 2-(3,4-dihydroxyphenyl)-5-hydroxy-4-oxo-4H-chromen-7- 7-olate luteolin-7-olate(1-) and the comparison ligand gefitinib, with the EGFR protein as an inhibitor. The results of the molecular dynamics simulation include RMSD (Root Mean Square Deviation), RMSF (Root Mean Square Fluctuation), and the total binding energy obtained using the Molecular Mechanics Generalized Born Surface Area (MM-GBSA) method. This simulation was performed with a timescale of 100 ns under constant temperature and pressure conditions.

Root Mean Square Deviation is the difference between the distance and conformation of the test ligand and the distance and conformation of the reference ligand [28]. RMSD analysis aims to ensure the stability of complex protein and ligand structures. The RMSD data is presented in a graph showing the RMSD values in angstroms (Å) between the reference ligand and the test ligand, as seen in Figure 3.

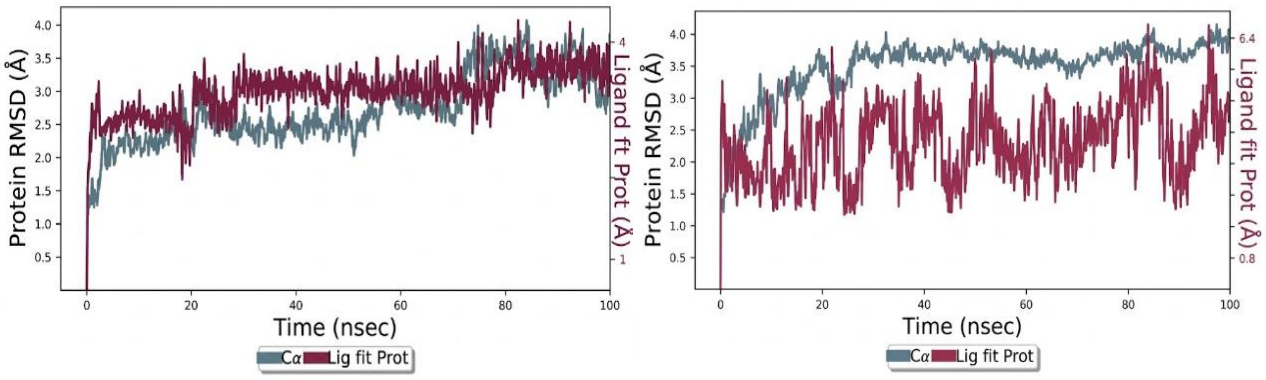

(a) (b)

Fig. 3: RMSD Values of Gefitinib – 4WKQ (a) and RMSD Values of the Best Test Ligand – 4WKQ (b)

In the simulation conducted over 100 nanoseconds, both compounds showed an increase in backbone RMSD, indicating that the protein structure began to unfold. The RMSD for the reference ligand gefitinib 4WKQ began to stabilize after 20 to 80 nanoseconds, then started to increase again after 80 to 100 nanoseconds. In contrast, the RMSD for the test ligand 22-(3,4-dihydroxyphenyl)-5-hydroxy-4-oxo-4H-chromen-7-olate luteolin- 7-olate(1-) – 4WKQ began to stabilize after 0 to 20 nanoseconds, then started to increase again after 20 to 25 nanoseconds, then stabilized again until 75 nanoseconds, and finally increased again after 75 to 100 nanoseconds. An increase in the RMSD value suggests that the receptor structure is beginning to open and the ligand is starting to hunt for acceptable binding sites or locations on the protein [29]. Based on Figure 3, the molecular dynamics simulation results show that the RMSD value of the reference ligand gefitinib 4WKQ is in the range of 3.4–4 Å, and the test ligand 2-(3,4-dihydroxyphenyl)-5-hydroxy-4-oxo-4H- chromen-7-olate luteolin-7-olate(1-) 4WKQ is in the range of 3.2–3.7 Å. From these results, the RMSD value range of the test ligand is lower than that of the reference ligand. The graph of the test ligand 2-(3,4- dihydroxyphenyl)-5-hydroxy-4-oxo-4H-chromen -7-olate luteolin-7-olate(1-) is more stable than the graph of the reference ligand Gefitinib. A stable RMSD value indicates that the optimal conformation of the protein bound to the ligand has been achieved, allowing the protein to maintain its position. The lower RMSD fluctuation observed for the selected compound suggests improved conformational stability of the ligand–EGFR complex during simulation, indicating a potentially more stable interaction within the receptor binding pocket. In addition, the interaction between residues also helps the protein maintain its structural stability [29].

Root Mean Fluctuation

RMSF is one of the important parameters for evaluating the fluctuations resulting from the interaction between ligands and amino acids in proteins during simulations. Unlike RMSD, which measures overall positional changes, RMSF focuses on the fluctuations of each protein residue, analyzing the extent to which each residue moves during the simulation. In other words, the RMSF value provides a clear picture of the flexibility of ligand interactions with each amino acid residue, reflecting the dynamics and stability of the protein structure within the context of the intertwined bonds [30]. The RMSF values between the test ligand and the reference ligand can be seen in Figure 4.

From Figure 4, it can be seen that the fluctuations can indicate the flexibility of the amino acid, which can be influenced by the type of ligand interacting with the receptor. In the reference ligand gefitinib 4WKQ, high fluctuations were observed in the amino acids Met 793, Gln 791, and Thr 854, indicating slight instability in the bonds formed at these amino acids. In contrast, in the test ligand 2-(3,4-dihydroxyphenyl)-5-hydroxy-4-oxo-4H-chromen-7- olate luteolin-7olate(1-) – 4WKQ, high fluctuations were observed only at the amino acid Met 793.

Visualization of Molecular Dynamics

The 2D visualization results are needed to understand the amino acid bonds formed during the molecular dynamics simulation and compare them with the results of the molecular docking simulation. The 2D visualization of the best test ligand and the comparison test ligand, gefitinib, with the EGFR protein (4WKQ) from molecular docking and molecular dynamics results can be seen in Figures 5 and 6.

DOI: 10.3844/ojbsci.2026.26.03.060

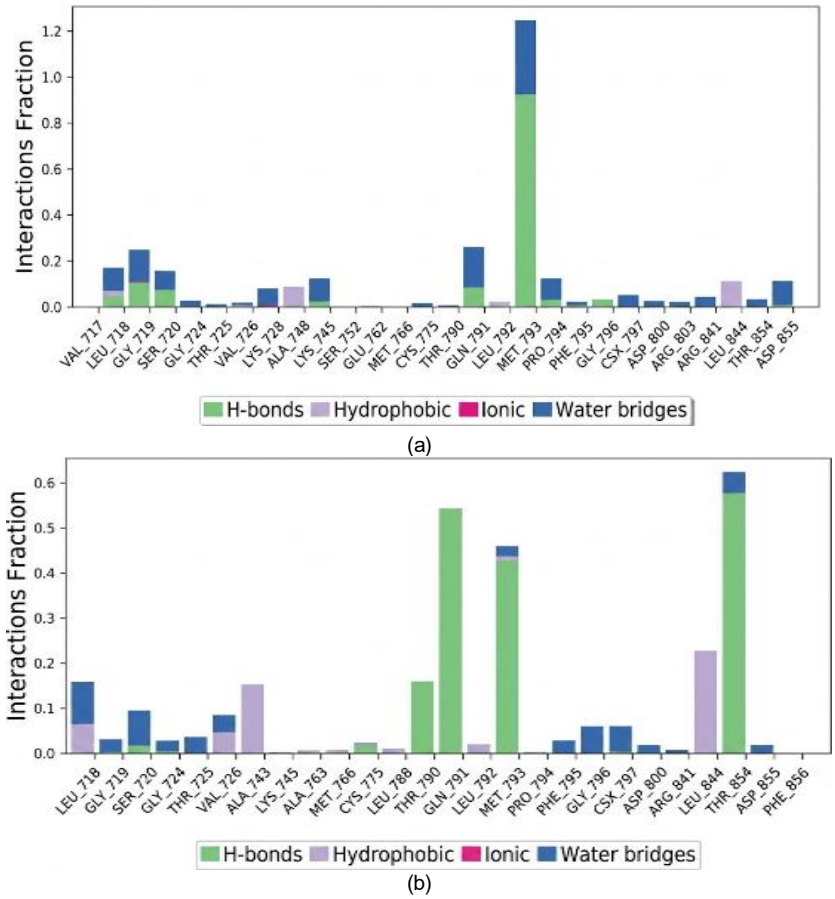

Fig. 4: RMSF values for Gefitinib – 4WKQ (a) and the best test ligand – 4WKQ (b)

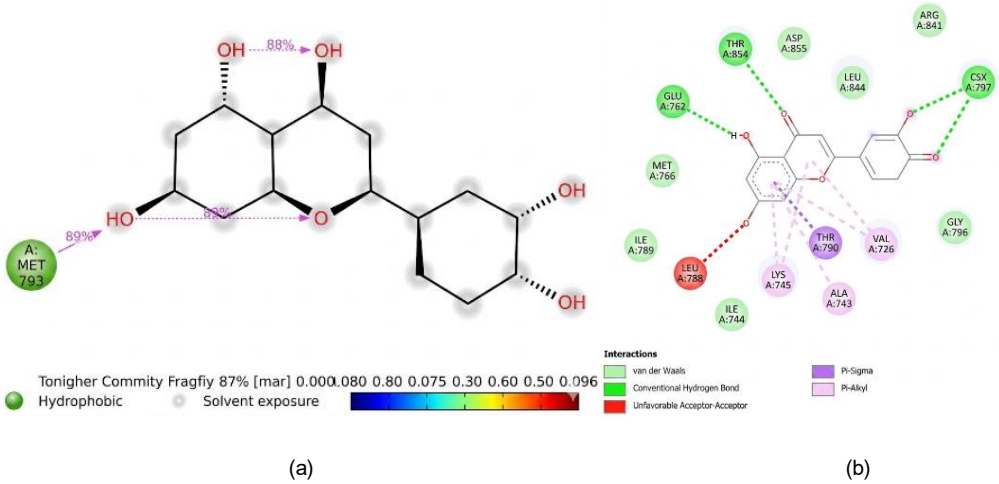

Fig. 5: The 2D visualization of the best test ligand from molecular docking (a) and molecular dynamics (b)

In the ligand complex of the test compound 2-(3,4-dihydroxyphenyl)-5-hydroxy-4-oxo-4H-chromen-7-olate luteolin-7-olate(1-), there is a significant difference in the amino acids, as shown in Figure 5. The amino acids in the molecular docking results, which initially included 7 amino acids, namely, Thr 854, Glu 762, Csx 797, Val 726, Ala 743, Lys 745, and Thr 790. After molecular dynamics, there was 1 remaining amino acid residue, Met 793. In the molecular dynamics simulation, more than 30% of interactions occurred from 0 to 100 nanoseconds.

DOI: 10.3844/ojbsci.2026.26.03.060

Based on Figure 6, it can be seen that there is a change in the interaction between the results of the molecular docking simulation and the results after molecular dynamics is performed. For the reference ligand gefitinib, the molecular docking interaction results showed 14 amino acids, including Met 793, Gln 791, Thr 854, Asp 800, Pro 794, Met 766, Leu 788, Lys 745, Val 726, Leu 792, Leu 718, Leu 844, Ala 743, and Glu 762. However, only 3 amino acids remained after molecular dynamics simulation, namely Met 793, Gln 791, and Thr 854. The molecular dynamics results between the best test ligand and the comparison test ligand, gefitinib, show that the test ligand is superior to the comparison ligand. This is because both the test ligand and the comparison ligand have hydrophobic bonds with the same amino acid, Met 793. Although the test ligand only has 1 amino acid residue interacting with the EGFR protein (4WKQ), its interaction is better (89%) than that of the comparison ligand gefitinib (42%).

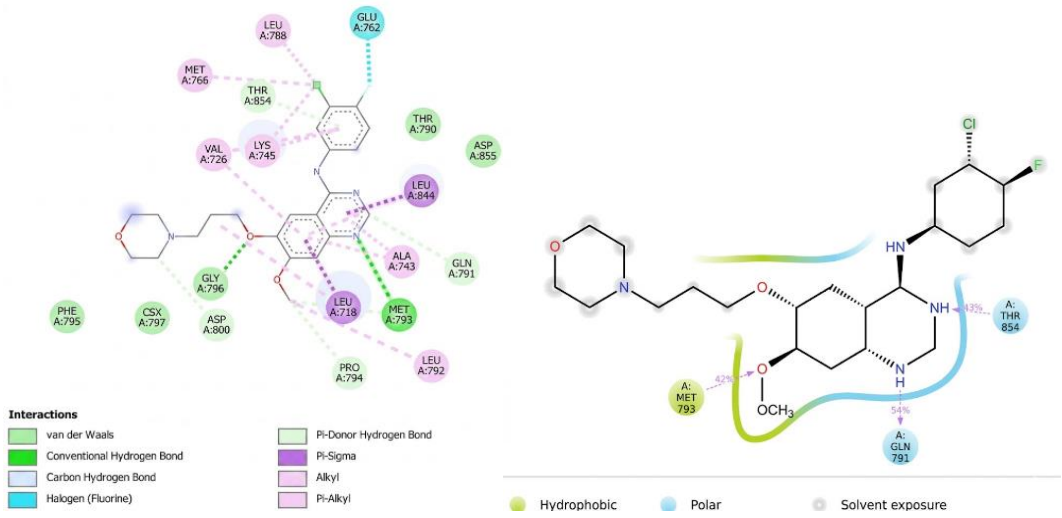

(a) (b)

Fig. 6: The 2D visualization of the reference ligand gefitinib resulting from molecular docking (a) and molecular dynamics (b)

The Molecular Mechanics Generalized Born Surface Area method is a common way to find the free binding energy (ΔG) in ligand-receptor systems [31]. The increasing free energy value indicates the compound's ability to bind with the receptor. The total energy between the test ligand 2-(3,4-dihydroxyphenyl)-5-hydroxy-4-oxo- 4H-chromen-7-olate luteolin-7-olate(1-) + 4WKQ (22.69 kcal/mol) is lower than that of the comparison ligand gefitinib + 4WKQ (41.82 kcal/mol). The total energy results for both the test ligand and the reference ligand showed positive values, while the total energy analysis between the receptor and the ligand should yield negative values to indicate the desired stability. This positive value indicates that the interaction between the test ligand and the reference ligand is less stable when the protein-ligand complex is formed. This situation may be caused by inaccuracies in the calculation of non-bonded energy, as well as the presence of other factors that can influence the results, such as the simulation environment or the parameters used in the model [31]. The lower MM-GBSA energy value obtained for the selected compound compared with gefitinib suggests relatively more favorable interaction stability; however, the positive energy values indicate that these findings should be interpreted cautiously and require further validation.

Conclusion

Based on the research, the test ligand 2-(3,4-dihydroxyphenyl)-5-hydroxy-4-oxo-4H-chromen -7-olate luteolin-7- olate(1-) from Allium sativum L. has a binding affinity of -8.8 kcal/mol and an inhibition constant of 0.966 μM, which is better than gefitinib (-7.9 kcal/mol, 0.970 μM). This ligand has good physicochemical properties, a toxicity class of 6, is non-mutagenic, and is non-toxic to the liver, while gefitinib is potentially toxic to the liver. The ADME profiles of the test ligand and gefitinib showed good quality, with a strong structure-activity relationship. The test ligand is predicted to inhibit EGFR with a total free energy of 22.69 kcal/mol, which is better than gefitinib (41.82 kcal/mol), indicating great potential in inhibiting EGFR with a stable ligand-receptor complex.

Acknowledgment

The authors express their gratitude to the Sekolah Tinggi Teknologi Industri dan Farmasi Bogor for providing facilities for in silico testing. They also thank Dr. Achamad Fauzi Isa for his recommendations and corrections to this study.

Funding Information

The Sekolah Tinggi Teknologi Industri dan Farmasi Bogor provided funding for this study.

Author's Contributions

Dinda Ratu Agustiani: Concept, manuscript writing, critical revision of the manuscript, data collection.
Rakhmat Ramdhani Alwie: Data analysis.
Harry Noviardi: Concept, manuscript writing, critical revision of the manuscript, data collection, final approval.

Ethics

The authors confirm that there are no conflicts of interest regarding the publication of this article. All of them have reviewed and approved the final version of the manuscript. This study did not include human participants or animal experiments.

References

1. Zumla, A., Valdoleiros, S. R., Haider, N., Asogun, D., Ntoumi, F., Petersen, E., & Kock, R. (2022). Monkeypox outbreaks outside endemic regions: scientific and social priorities. The Lancet Infectious Diseases, 22(7), 929–931. https://doi.org/10.1016/s1473-3099(22)00354-1
2. Carrubba, S., Geevarghese, A., Solli, E., Guttha, S., Sims, J., Sperber, L., Meehan, S., & Ostrovsky, A. (2023). Novel severe oculocutaneous manifestations of human monkeypox virus infection and their historical analogues. In The Lancet Infectious Diseases (Vol. 23, Issue 5, pp. e190–e197). https://doi.org/10.1016/s1473-3099(22)00869-6
3. Doty, J., Malekani, J., Kalemba, L., Stanley, W., Monroe, B., Nakazawa, Y., Mauldin, M., Bakambana, T., Liyandja Dja Liyandja, T., Braden, Z., Wallace, R., Malekani, D., McCollum, A., Gallardo-Romero, N., Kondas, A., Peterson, A., Osorio, J., Rocke, T., Karem, K., … Carroll, D. (2017). Assessing Monkeypox Virus Prevalence in Small Mammals at the Human–Animal Interface in the Democratic Republic of the Congo. In Viruses (Vol. 9, Issue 10, p. 283). https://doi.org/10.3390/v9100283
4. Alakunle, E. F., & Okeke, M. I. (2022). Monkeypox virus: a neglected zoonotic pathogen spreads globally. In Nature Reviews Microbiology (Vol. 20, Issue 9, pp. 507–508). https://doi.org/10.1038/s41579-022-00776-z
5. Patauner, F., Gallo, R., & Durante-Mangoni, E. (2022). Monkeypox infection: An update for the practicing physician. European Journal of Internal Medicine, 104, 1–6. https://doi.org/10.1016/j.ejim.2022.08.022
6. Murphrey, M. B., Quaim, L., Rahimi, N., & Varacallo, M. A. (2025). Biochemistry, Epidermal Growth Factor Receptor. StatPearls, NBK482459.
7. Adler, H., Gould, S., Hine, P., Snell, L. B., Wong, W., Houlihan, C. F., Osborne, J. C., Rampling, T., Beadsworth, M. B., Duncan, C. J., & Dunning, J. (2022). Clinical features and management of human monkeypox: a retrospective observational study in the UK. The Lancet Infectious Diseases, 22(8), 1153–1162. https://doi.org/10.1016/S1473-3099(22)00228-6
8. Kobayashi, R., Hoshikawa, E., Saito, T., Suebsamarn, O., Naito, E., Suzuki, A., Ishihara, S., Haga, H., Tomihara, K., & Izumi, K. (2023). The EGF/EGFR axis and its downstream signaling pathways regulate the motility and proliferation of cultured oral keratinocytes. In FEBS Open Bio (Vol. 13, Issue 8, pp. 1469–1484). https://doi.org/10.1002/2211-5463.13653
9. Xu, X., Huang, M., & Zou, X. (2018). Docking-based inverse virtual screening: methods, applications, and challenges. Biophysics Reports, 4(1), 1–16. https://doi.org/10.1007/s41048-017-0045-8
10. Lengbiye, E. M., Mbadiko, C. M., Falanga, C. M., Matondo, A., Inkoto, C. L., Ngoyi, E. M., Kabengele, C. N., Bongo, G. N., Gbolo, B. Z., Kilembe, J. T., Mwanangombo, D. T., Tshibangu, D. S. T., Tshilanda, D. D., Mihigo, S. O., Ngbolua, K.-N., & Mpiana, P. T. (2020). Antiviral Activity, Phytochemistry and Toxicology of Some Medically Interesting Allium Species: A Mini Review. International Journal of Pathogen Research, 5(4), 64–77. https://doi.org/10.9734/ijpr/2020/v5i430145
11. Nath, R., Singha, S., Nath, D., Das, G., Patra, J., & Talukdar, A. (2022). Phytochemicals from Allium tuberosum Rottler ex Spreng Show Potent Inhibitory Activity against B-Raf, EGFR, K-Ras, and PI3K of Non-Small Cell Lung Cancer Targets. Applied Sciences, 12(22), 11749. https://doi.org/10.3390/app122211749
12. Tambunan, U. S. F., Nasution, M. A. F., Parikesit, A. A., Noviardi, H., & Kerami, D. (2016). Designing of Disulfide Cyclic Peptide for Inhibiting Polymerase A and B1 (PAC-PB1N) in H1N1 Virus using Molecular Simulation Approach. OnLine Journal of Biological Sciences, 16(3), 122–129. https://doi.org/10.3844/ojbsci.2016.122.129
13. Wulanawati, A., Noviardi, H., & Ibrohim, M. S. M. (2018). Finding a Potential Bruceine D Inhibitor for Apoptotic Resistance Protein Pancreatic Cancer Based on Molecular Docking. Indonesian Journal of Chemistry, 18(3), 566. https://doi.org/10.22146/ijc.25220

14. Trott, O., & Olson, A. J. (2010). AutoDock Vina: Improving the Speed and Accuracy of Docking with a New Scoring Function, Efficient Optimization, and Multithreading. Journal of Computational Chemistry, 31(2), 455–461. https://doi.org/10.1002/jcc.21334
15. Yuningtyas, S., Alfarabi, M., Lestari, Y., & Noviardi, H. (2024). The In Vitro and In Silico Study of α-glucosidase Inhibition by Kombucha Derived from Syzygium polyanthum (Wight) Walp. Leaves. HAYATI Journal of Biosciences, 31(5), 951–963. https://doi.org/10.4308/hjb.31.5.951-963
16. Pires, D. E. V., Blundell, T. L., & Ascher, D. B. (2015). pkCSM: Predicting Small-Molecule Pharmacokinetic and Toxicity Properties Using Graph-Based Signatures. Journal of Medicinal Chemistry, 58(9), 4066–4072. https://doi.org/10.1021/acs.jmedchem.5b00104
17. Pal, P., Thummuri, D., Lv, D., Liu, X., Zhang, P., Hu, W., Poddar, S. K., Hua, N., Khan, S., Yuan, Y., Zhang, X., Zhou, D., & Zheng, G. (2021). Discovery of a Novel BCL-XL PROTAC Degrader with Enhanced BCL-2 Inhibition. Journal of Medicinal Chemistry, 64(19), 14230–14246. https://doi.org/10.1021/acs.jmedchem.1c00517
18. Noviardi, H., Iswantini, D., Mulijani, S., Wahyudi, S. T., Khusniati, T., & Sulistiani, S. (2023). Anti-inflammatory activity of the metabolite extract of Lactobacillus plantarum Su-ls29 on lipopolysaccharide-induced RAW 264.7 macrophage cells. Journal of Applied Pharmaceutical Science, 14(1), 148–158. https://doi.org/10.7324/japs.2024.141691
19. Agnihotry, S., Pathak, R. K., Singh, D. B., Tiwari, A., & Hussain, I. (2022). Chapter 11 - Protein Structure Prediction. Bioinformatics, 177–188. https://doi.org/10.1016/b978-0-323-89775-4.00023-7
20. Beerli, C., Yakimovich, A., Kilcher, S., Reynoso, G. V., Fläschner, G., Müller, D. J., Hickman, H. D., & Mercer, J. (2018). Vaccinia virus hijacks EGFR signalling to enhance virus spread through rapid and directed infected cell motility. In Nature Microbiology (Vol. 4, Issue 2, pp. 216–225). https://doi.org/10.1038/s41564-018-0288-2
21. Noviardi, H., Yuningtyas, S., Adzani, A., & Alawiyah, R. M. (2025). Antioxidant and Antidiabetic Activities of Manalagi Apple (Malus sylvestris Mill) Juice and Water Kefir: An *in vitro* and In Silico Study. Tropical Journal of Natural Product Research, 9(11), 5520–5528. https://doi.org/10.26538/tjnpr/v9i11.35
22. Tallei, T. E., Tumilaar, S. G., Niode, N. J., Fatimawali, Kepel, B. J., Idroes, R., Effendi, Y., Sakib, S. A., & Emran, T. B. (2020). Potential of Plant Bioactive Compounds as SARS-CoV-2 Main Protease (Mpro) and Spike (S) Glycoprotein Inhibitors: A Molecular Docking Study. Scientifica, 2020, 1–18. https://doi.org/10.1155/2020/6307457
23. Nhlapho, S., Nyathi, M., Ngwenya, B., Dube, T., Telukdarie, A., Munien, I., Vermeulen, A., & Chude-Okonkwo, U. (2024). Druggability of Pharmaceutical Compounds Using Lipinski Rules with Machine Learning. Sciences of Pharmacy, 3(4), 177–192. https://doi.org/10.58920/sciphar0304264
24. Chander, S., Tang, C.-R., Al-Maqtari, H. M., Jamalis, J., Penta, A., Hadda, T. B., Sirat, H. M., Zheng, Y.-T., & Sankaranarayanan, M. (2017). Synthesis and study of anti-HIV-1 RT activity of 5-benzoyl-4-methyl-1,3,4,5-tetrahydro- 2H -1,5-benzodiazepin-2-one derivatives. In Bioorganic Chemistry (Vol. 72, pp. 74–79). https://doi.org/10.1016/j.bioorg.2017.03.013
25. Moorthy, N. S. H. N., Ramos, M. J., & Fernandes, P. A. (2011). Structural analysis of α-glucosidase inhibitors by validated QSAR models using topological and hydrophobicity based descriptors. Chemometrics and Intelligent Laboratory Systems, 109(2), 101–112. https://doi.org/10.1016/j.chemolab.2011.02.010
26. Puttaswamy, H., Gowtham, H. G., Ojha, M. D., Yadav, A., Choudhir, G., Raguraman, V., Kongkham, B., Selvaraju, K., Shareef, S., Gehlot, P., Ahamed, F., & Chauhan, L. (2020). In silico studies evidenced the role of structurally diverse plant secondary metabolites in reducing SARS-CoV-2 pathogenesis. Scientific Reports, 10(1), 20584. https://doi.org/10.1038/s41598-020-77602-0
27. Salo-Ahen, O. M. H., Alanko, I., Bhadane, R., Bonvin, A. M. J. J., Honorato, R. V., Hossain, S., Juffer, A. H., Kabedev, A., Lahtela-Kakkonen, M., Larsen, A. S., Lescrinier, E., Marimuthu, P., Mirza, M. U., Mustafa, G., Nunes-Alves, A., Pantsar, T., Saadabadi, A., Singaravelu, K., & Vanmeert, M. (2020). Molecular Dynamics Simulations in Drug Discovery and Pharmaceutical Development. Processes, 9(1), 71. https://doi.org/10.3390/pr9010071
28. Puratchikody, A., Sriram, D., Umamaheswari, A., & Irfan, N. (2016). 3-D structural interactions and quantitative structural toxicity studies of tyrosine derivatives intended for safe potent inflammation treatment. Chemistry Central Journal, 10(1), 24. https://doi.org/10.1186/s13065-016-0169-9
29. Dinata, D. I. (2023). Identification of angiotensin receptor blocker II ligands from Gotu Kola (Centella asiatica L.) extract: an in silico study. *Indonesian Journal of Pharmaceutical Science and Technology*, 5(2),196-206. https://doi.org/10.24198/ijpst.v0i0.50346
30. Rosa, R. S. de L., Bulla, A. C. S., Bernardi, R. C., & Leal da Silva, M. (2025). Impact of Structural Relaxation on Protein–Protein Docking in Large Macromolecular Complexes. Applied Biosciences, 4(4), 48. https://doi.org/10.3390/applbiosci4040048
31. Genheden, S., & Ryde, U. (2015). The MM/PBSA and MM/GBSA methods to estimate ligand-binding affinities. Expert Opinion on Drug Discovery, 10(5), 449–461. https://doi.org/10.1517/17460441.2015.1032936